RSC Advances

PAPER

View Article Online
View Journal | View Issue

Cite this: RSC Adv., 2015, 5, 31852

Tautomeric transformations of piroxicam in solution: a combined experimental and theoretical study†

D. Ivanova,[ab] V. Deneva,[a] D. Nedeltcheva,*[a] F. S. Kamounah,[c] G. Gergov,[b] P. E. Hansen,[c] S. Kawauchi[d] and L. Antonov[a]

Received 1st March 2015
Accepted 24th March 2015

DOI: 10.1039/c5ra03653d

www.rsc.org/advances

Piroxicam tautomerism was studied in solution by using UV-Vis spectroscopy, NMR measurements and advanced chemometrics. It has been found that in ethanol and DMSO the enol-amide tautomer is present mainly as a sandwich type dimer. The addition of water leads to distortion of the aggregate and to gradual shift of the equilibrium towards the zwitterionic tautomer. Quantitative data for the aggregation and the tautomeric equilibria are presented. Quantum chemical calculations (M06-2X/TZVP) have been used to explain stability of the tautomers as a function of the solvent and concentration.

Introduction

Non-steroidal anti-inflammatory drugs (NSAIDs) exert their pharmacological effect chiefly by inhibition of the enzyme cyclooxygenase, which catalyzes the rate-limiting step of prostaglandin synthesis.[1] Piroxicam (Px), which effectiveness against various inflammatory conditions such as osteoarthritis, rheumatoid arthritis and ankylosing spondylitis[2] is well documented, belongs to the oxicam group of NSAIDs. In recent years Px has been subject to renewed interest due to accumulation of experimental data about potential chemoprevention properties against colorectal cancer.[3] However, in addition to these therapeutic actions, Px causes certain characteristic undesirable reactions, of which gastrotoxicity and photosensitivity have been the most frequently observed.[4] Such a wide spectrum of physiological effects and their correlation to the structural characteristics of the drug molecule establish the importance of investigating the variations in the chemical structure in different environments.

In addition, Px exhibits rich tautomeric behavior attracting attention from both fundamental and practical viewpoints.[5–7] As seen from Fig. 1, Piroxicam can exist in 7 different tautomeric forms and the conversion between them is important for its delivery and action[8] since only the neutral form of oxicam drugs is suggested to be biologically active.[9] Resulting from the Px poor water solubility,[10] it is worth mentioning that Px tautomerism has been mainly investigated in the light of forming soluble co-crystals with carboxylic acids and other pharmaceutically acceptable organic compounds aimed towards increased bioavailability.[11,12] There is scattered information about Px tautomerism in neutral state in solution: in solvents without hydrogen bonding abilities the enol (PxA) dominates[13,14] and clear concentration and pH behavior has been reported in alcohols.[6] The experimental findings have been supported by theoretical studies showing the importance of the solvent environment.[15]

In most of these cases there are no quantitative data for the position of the tautomeric equilibrium obtained from the spectral data. One possibility to obtain quantitative information about the tautomers is the use of advanced chemometric procedures that allow extraction of individual spectra of the tautomers from the complicated spectral envelopes.[16] Another option is to use low temperature NMR spectra.[17] Geckle *et al.* found in DMF-d_7 at 205 K that the main form is the PxA in slow exchange with a minor form, 19% at that temperature. They assigned the minor form to be the zwitterionic form (PxZw) based on comparison with solid state NMR spectra. The later may also provide ^{13}C NMR chemical shift values of different polymorphisms.[18] Furthermore, NMR, especially the use of deuterium isotope effects on ^{13}C chemical shifts, provides a strong tool for determining the presence of a tautomeric equilibrium and the structure of the equilibrating species.[19,20] The aim of the current study is to provide quantitative information about the Px tautomerism as a function of solvent and concentration and to connect this data with the quantum chemical calculations.

[a]Institute of Organic Chemistry with Centre of Phytochemistry, Bulgarian Academy of Sciences, Acad. G. Bonchev str., bldg. 9, BG-1113 Sofia, Bulgaria. E-mail: dantonova@orgchm.bas.bg

[b]Faculty of Pharmacy, Medical University of Sofia, 2 Dunav str., BG-1000 Sofia, Bulgaria

[c]Department of Science, Systems and Models, Roskilde University, P.O. Box 260, DK-4000 Roskilde, Denmark

[d]Tokyo Institute of Technology, Department of Organic and Polymeric Materials, 2-12-1 O-okayama, Meguro-ku, Tokyo 152-8552, Japan

† Electronic supplementary information (ESI) available: See DOI: 10.1039/c5ra03653d

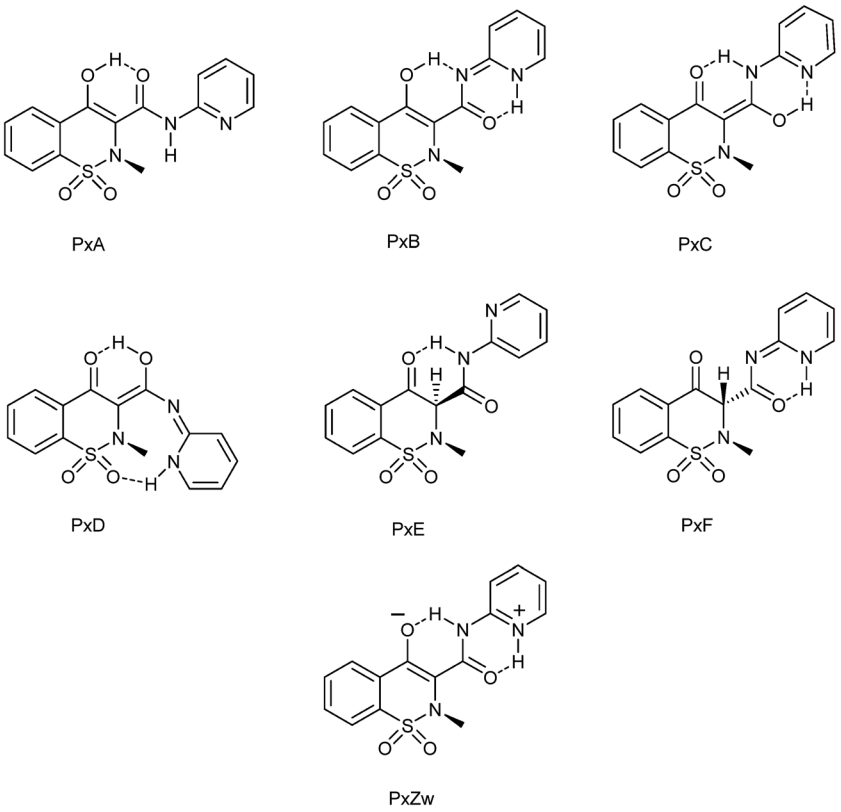

Fig. 1 The most stable conformations of the tautomeric forms of Px according to the quantum-chemical results (M06-2X/TZVP).

Results and discussion

As mentioned above, seven neutral Px tautomers are generally possible, each of them existing as a number of isomers stabilized by a combination of intramolecular hydrogen bonds. According to the quantum-chemical calculations in ethanol and water, both solvents presented as a continuum, the enol-amide form PxA is the most stable one. The other energetically similar tautomers are presented in Fig. 2 and information on the most stable isomers of the corresponding tautomers is compiled in Table 1. The energies in gas phase, ethanol and water for all possible isomers are presented in Tables S1–S3.† In Fig. S1–S3† the data are summarized graphically.

According to Fig. 2, the zwitterionic structure PxZw is strongly stabilized by water environment, but not enough to be considered actually present in solution. The enol-imide tautomer PxB and the keto-amino form PxC are the other two most stable structures. It is interesting to point out that these three forms exhibit the same stabilizing hydrogen bonding network, which limits interactions with proton acceptor solvents and intermolecular hydrogen bonding as a whole.

The absorption spectra of Px in ethanol as functions of the concentration are shown in Fig. 3. Evidently, the spectral changes are strongly concentration dependent: upon dilution the maximum at 325 nm decreases and absorption rises in the region 350–400 nm. This behavior assumes an aggregation process and the presence of a clear isobestic point suggests that a monomer–dimer equilibrium ($2M \rightleftarrows D$) is at play, where the monomer is the PxA tautomeric form as proven above by the theoretical calculations and previous experimental studies.[5] The spectral data were analysed by using the methodology, previously developed by us,[21] and the obtained dimerization constant is shown in Table 2. It is clear that the dimer is dominating (almost 97%) in the most concentrated solution (5×10^{-4} M), while upon dilution a weak monomer peak at 363 nm appears. However, the dimerization is very strong and even after dilution three orders of magnitude (8.0×10^{-7} M) the monomer fraction is only around 60%. The spectrum of the dimer exhibits two symmetric, with respect to the monomer, bands[22] – intensive H-band at 325 nm and very weak J-band at 395 nm. According to the exciton theory[21,22] this spectral structure suggests a sandwich-type dimer and the calculated angle between monomers transition dipole moments in the dimer (α in Table 2) shows almost an unidirectional arrangement.

A very similar concentration dependent spectral behavior was observed in DMSO (Fig. S4† and Table 2), where the aggregation is one order of magnitude weaker, but the structure of the dimer is essentially the same. Taking into account the nature of these two solvents (ethanol – proton acceptor and proton donor; DMSO – strong proton acceptor) and the stability of the dimer it could be expected that in the dimer structure the amide NH groups are available for interactions with the solvent molecules.

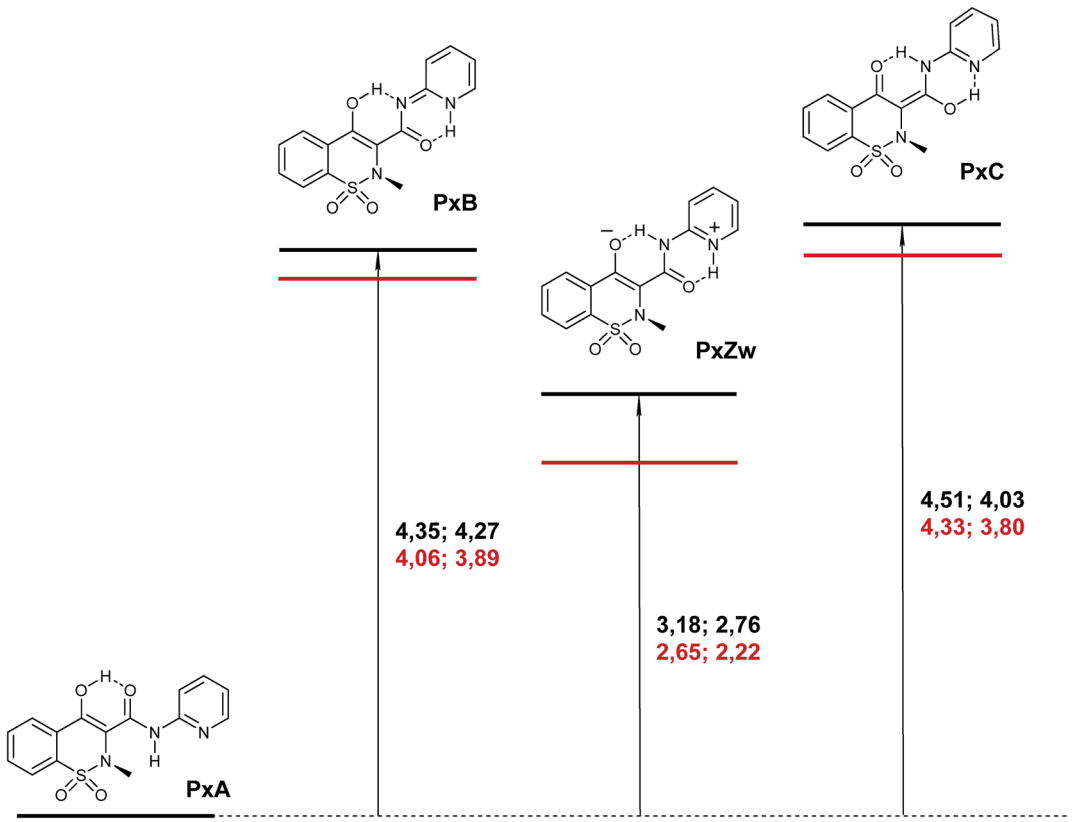

Fig. 2 Relative energies and Gibbs free energies (M06-2X/TZVP, in kcal mol^{-1} units) of the most stable structures in ethanol (black) and in water (red). The solvent is described by using the PCM model.

The theoretically predicted types of PxA dimers are presented in Fig. 4. It is worth emphasizing that the stabilization energies shown here are only rough estimations because the structures were optimized in an ethanol environment, which excludes basis set superposition error correction. In addition each of these three types of dimers exists as isomers, defined by the mutual position of the NMe group, whose energies are similar. Considering the structures from Fig. 4 and comparing them with monomeric PxA it could be suggested that D(NH···N) and D(SO···HN) do not provide conditions for intermolecular interaction with the solvent and they could be *a priori* destroyed by proton acceptor solvents such as DMSO. The D(SO···HO) dimer, where the NH groups are available for interactions with the solvent similarly to PxA itself, corresponds to the sandwich structure proven by the spectral data analysis as well. Additional arguments for its existence arise from the predicted spectral data given in Table 3. Only in the case of this structure two peaks are predicted, red and blue shifted, in respect to the PxA long-wavelength band and their relative intensity allows to calculate the angle $\alpha = 12°$, which corresponds well with the experimentally obtained value.

The discussion about D(SO···HO) existence has unexpected support coming from the ESI.† The analysis of the crystal

Table 1 Dipole moments (in D) and relative energies (in kcal mol^{-1}) of the most stable isomers of the corresponding tautomers of Px (as shown in Fig. 1) according to the quantum-chemical calculations (M06-2X/TZVP)

	Gas phase			Ethanol[a]			Water[a]		
Tautomer	μ	ΔE	ΔG	μ	ΔE	ΔG	μ	ΔE	ΔG
PxA	4.29	0.00	0.00	6.09	0.00	0.00	6.22	0.00	0.00
PxB	9.19	9.52	9.57	12.83	4.35	4.27	13.04	4.06	3.89
PxC	7.94	7.74	6.98	10.84	4.51	4.03	10.99	4.33	3.80
PxD	3.64	13.30	13.70	6.25	11.82	11.29	6.45	11.73	11.18
PxE	5.24	9.67	9.57	7.33	8.07	7.43	7.47	7.96	7.27
PxF	5.24	17.75	17.34	7.72	12.13	11.91	7.82	11.80	11.54
PxZw	11.45	13.42	11.68	16.12	3.18	2.76	16.32	2.65	2.22

[a] Solvent effect is described by using the PCM model.

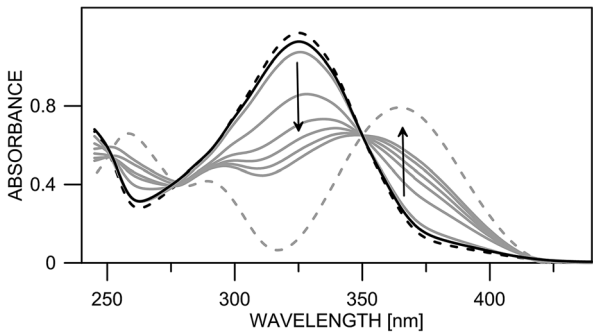

Fig. 3 Absorption spectra of Px in ethanol at various concentrations, keeping concentration × optical path length constant (5×10^{-5} M cm). The concentrations are as follows (solid lines) in black: 5.0×10^{-4} M (most concentrated); in gray (following arrow direction): 5.0×10^{-5} M, 5.0×10^{-6} M, 1.6×10^{-6} M, 1.2×10^{-6} M, 1.0×10^{-6} M, 8.0×10^{-7} M. Molar fractions of the monomer [%] are as follows: 4, 12, 31, 48, 53, 56, 60. Calculated spectra of dimer (black dashes) and of monomer (gray dashes).

Table 2 Parameters characterizing the monomer–dimer equilibrium as defined by the exciton theory,[22] estimated according to the procedure described in ref. 21

Solvent	$\log K_D$[a]	A[b] [°]	R[c] [Å]	λ_M[d] [nm]	λ_H[e] [nm]	λ_J[e] [nm]
Ethanol	5.86	17	3.4	363	325	395
DMSO	4.51	28	3.2	376	328	396

[a] Dimerization constant, defined as: $K_D = \frac{C_D}{C_M{}^2}$. [b] Angle between the transition dipole moments of the monomer molecules in the dimer. [c] Distance between monomer molecules in the dimer. [d] Position of the absorption maximum of the monomer. [e] Absorption maxima of the dimer (H and J denote blue and red shifted bands in respect of λ_M).

structures deposited in the ESI† has shown three polymorphs (I–III)‡ depending on the type of the formed hydrogen bonding networks: SO···HN§,[23,24] SO···HO¶[23,25,26] and SO···HC,[23] respectively. Structure I is practically identical with the D(SO···HN) dimer but as discussed above there is no proof of its presence in ethanol solution since, as described, it usually crystalizes from nonpolar solvents[26] or can be obtained by heating of electrosprayed piroxicam.[27] Structure II (Fig. 5), crystallizing from absolute ethanol solutions,[26] is very similar to D(SO···HO), but with a different relative position of the *N*-methyl groups. This difference is caused by the simplicity of the quantum chemical model, which considers only two PxA molecules without taking into account the hindrance of the methyl groups, while maximal packing is targeted in the crystal. It is worth noting that the optimized isomer with NMe groups positions as in the polymorph II is less stable compared to D(SO···HO) by only 0.08 kcal mol^{-1}, which is much below the frame of computational error. The predicted absorption spectrum of this isomer is essentially

‡ Recently a new polymorph was reported to be obtained by using electrospraying,[27] which recrystallizes completely into form I as a result of heating.
§ Called also β-piroxicam.
¶ Called also α-piroxicam.

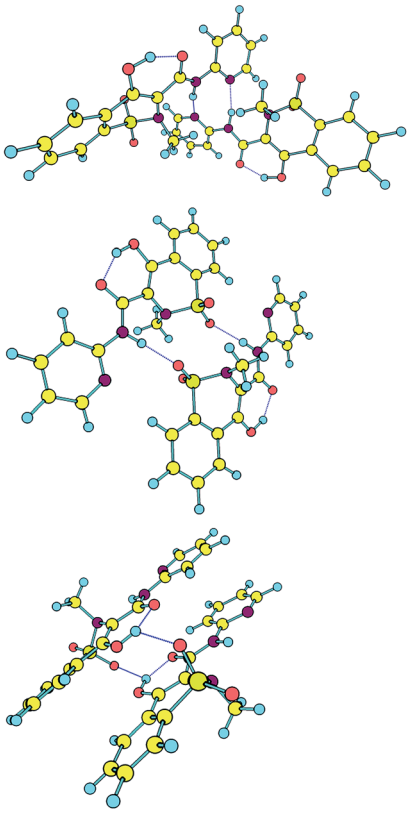

Fig. 4 Representative types of dimers of PxA (M06-2X/TZVP) in ethanol (PCM model) shown as the most stable isomers. Following values are shown below each structure: dipole moment, stabilization energy ($2E_{PxA} - E_D$) and stabilization Gibbs free energy ($2\Delta G_{PxA} - \Delta G_D$).

Table 3 Predicted (TD-DFT, M06-2X/TZVP) absorption maxima of the tautomers and dimers of Px. Solvent effect is described by using the PCM model

	Ethanol		Water	
Structure	λ_{max} [nm]	f[a]	λ_{max} [nm]	f[a]
PxA	294 (295)[b]	0.777 (0.792)[b]	294	0.771
PxB	317	0.798	317	0.791
PxC	322	0.606	322	0.600
PxD	341	0.528	340	0.527
PxE	238	0.510	237	0.509
PxF	284	0.430	284	0.430
PxZw	327	0.583	326	0.533
D(NH···N)	294 (295)[b]	1.046 (1.066)[b]	—	—
	292 (292)[b]	0.370 (0.380)[b]		
D(SO···HN)	298 (298)[b]	0.000 (0.000)[b]	—	—
	294 (295)[b]	1.396 (1.432)[b]		
D(SO···HO)	302 (305)[b]	0.014 (0.019)[b]	—	—
	292 (297)[b]	1.340 (1.391)[b]		

[a] Oscillator strength. [b] In DMSO.

the same: $\lambda_H = 292$ nm ($f = 1.332$) and $\lambda_J = 303$ nm ($f = 0.019$). In this way, both quantum-chemistry and the experiment agree almost perfectly, showing that the PxA exists mainly as an aggregate in solution.

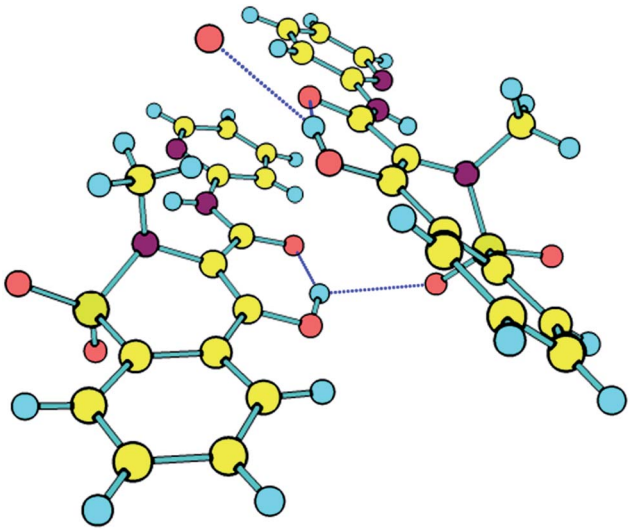

Fig. 5 Schematic presentation of the intermolecular interactions in polymorph II.[23,25]

The addition of water to the ethanol solution, as seen from Fig. 6, leads to spectral changes that require specific explanation. On the one hand, the absorption at 325 nm decreases suggesting a lowering of the dimer concentration in the solution. On the other hand, there is no clear isosbestic point to lead to conclusion that this process causes simple distortion of the dimer. The final spectrum, obtained at 80% water content differs substantially from the monomer spectrum. The derivative spectra also show complicated spectral behavior in the area between 350 and 400 nm. According to the quantum chemical calculations PxZw could be this new species, as will be shown below, stabilized by specific solute–solvent interactions with the water molecules. Additionally, the ESI† clearly shows that PxZw crystallizes from water-containing solutions.[25,28] In such a case, the dimer is not directly transformed into PxZw but through the initial generation of the enol monomer PxA, which is logical taking into account that the tautomeric transformation needs substantial structural re-arrangement:

$$\mathrm{D(SO\cdots HO)} \rightleftarrows \mathrm{PxA} \rightleftarrows \mathrm{PxZw}$$

The chemometric analysis of the spectral data[16,29] from Fig. 6 yields molar fractions of the species collected in Table 4. As seen, initial addition of water leads to shift of the equilibrium to the monomer. However, this change is not dramatic and eventually leads to almost constant dimer/monomer ratio in response of the changed environment. The water molecules probably do not destroy directly the dimer, but gradually replace ethanol ones at the possible interaction sites. At the same time, the increased water content leads to stabilization of the PxZw and the gradual increase in its concentration in the solution (Fig. S5†), which finally shifts the equilibrium from the dimer to the zwitterionic species. Similar spectral behavior has been observed in DMSO–water mixtures (Fig. S6 and S7†). Owing to the lower stability of the dimer in DMSO the PxZw in this case appears at much lower water content but similarly the dimer/monomer ratio reaches stabilization. The tautomeric constants are higher compared to the ethanol–water mixtures, which can be attributed to the higher dielectric constant of DMSO in addition to the lower dimer stability.

The transformation of PxA to PxZw finds evidence in the obtained NMR results. Due to low solubility of Px in most of the solvents, three types of NMR experiments have been performed in this study: (i) addition of water to solutions of Px in DMSO-d_6; (ii) measurement of deuterium isotope effects on ^{13}C chemical shifts by addition of small amounts of D_2O to solutions in DMSO-d_6 or (iii) attempts to measure deuterium isotope effects on ^{13}C chemical shifts of partially deuterated Px in DMF-d_7 at low temperature.

The latter experiment gave no resolvable results as the lines are broad. Addition of 5 μL D_2O respectively 5 μL H_2O gave the isotope effects as seen in Table 5. The isotope effects are plotted *vs.* the difference in ^{13}C chemical shifts between PxA and PxZw as taken from ref. 17. The results for C-7, C-9, C-11 and C-12 (atom numbering as in ref. 17, Fig. 7) are seen to fall off the correlation line. This can be interpreted in the following way. If an equilibrium exists between the PxA and the PxZw forms, then isotope effects will be a combination of an intrinsic and an equilibrium part and the difference in chemical shifts will be proportional[19,20] for carbons close to the sites of deuteriation the intrinsic effect exist, whereas for those carbons far from the site of deuteriation the intrinsic effects will be small and the equilibrium effect will dominate. This means that the isotope effect will be proportional to the difference in ^{13}C chemical shifts of the two tautomers.[19,20] This picture is clearly seen in Fig. 7. Carbons C-7, C-9, C-11 and C-12 are close to the sites of deuteriation and are falling off the correlation line. For the two

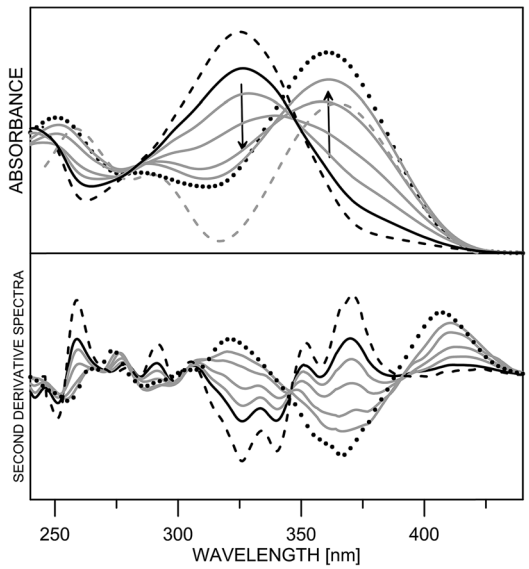

Fig. 6 Absorption spectra of Px in ethanol with addition of water: (a) zero order spectra from 0% water (black solid line) to 80% water (dots); (b) corresponding second derivative spectra. The water content is given in Table 4, the curve with 5% water is omitted. The spectra of the monomer (gray dashes) and dimer (black dashes) of PxA are given for comparison.

Table 4 Molar fractions [%] of the mixture components as function of the water content

	Ethanol					DMSO				
	Molar fraction					Molar fraction				
Water $[\%]_v$	D(SO···HO)	PxA	PxZw	K_T[a]	log K_D	D(SO···HO)	PxA	PxZw	K_T[a]	log K_D
0	89	11	0	—	5.86	84	16	0	—	4.51
5	78	22	0	—	5.20	58	37	5	0.05	3.62
10	66	33	1	0.01	4.78	47	38	15	0.17	3.51
20	47	41	12	0.13	4.44	33	39	28	0.38	3.33
40	26	46	28	0.38	4.08	14	25	61	1.56	3.25
60	14	36	50	1.00	4.03	5	15	80	4.00	3.34
80	4	18	78	3.54	4.09	0	4	96	24.0	—

[a] Defined as [PxZw]/[PxA + D(SO···HO)] ratio.

Table 5 Deuterium isotope effects on ^{13}C chemical shifts of piroxicam

Carbon atom	In DMSO-d_6 + 5 mL H_2O	In DMSO-d_6 + 5 mL D_2O	
C-9	166.92	166.70	0.22
C-7	160.32	159.79	0.53
C-11	150.13	150.02	0.11
C-15	145.60	145.89	−0.29
C-13	140.06	139.82	0.24
C-1	134.77	134.73	0.04
C-4	133.24	133.27	−0.03
C-3	132.70	132.75	−0.05
C-6	129.48	129.31	0.17
C-5	126.59	126.50	0.02
C-2	123.89	123.93	−0.04
C-14	120.04	120.14	−0.1
C-12	116.33	116.19	0.14
C-8	110.82	110.87	−0.05

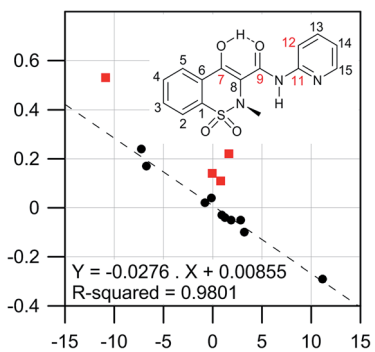

Fig. 7 Plot of difference in ^{13}C chemical shifts between the PxA and PxZw forms (see text) *vs.* deuterium isotope effects on ^{13}C chemical shifts (the data for C-7, C-9, C-11 and C-12 are given in red squares).

latter the intrinsic effects are smaller as the proportion of the other form is small. However, the fact that C-11 and C-12 are involved clearly shows that the pyridine nitrogen is protonated and that the other tautomer is PxZw.

By addition of water we find a linear correlation between the ^{13}C chemical shift and the amount of water (Fig. S8†). The chemical shifts move in the direction of the PxZw form. A correlation between the difference in chemical shifts of the ^{13}C chemical shifts of the PxA and PxZw forms (see previously) and the difference between in chemical shifts between no water and 40 μL water added. This again shows that the PxZw form is at play. The outlier is C-6, which is close to C-7 which in the PxZw form is substituted with O^-. The deviation can be understood as a water molecule binding to the O^- site.

An attempt for a detailed picture of how water interacts with PxA and PxZw forms comes from the possible specific water–PxA and water–PxZw interactions following a bottom-up procedure starting from isolated tautomers (Table S4†). Initially, the first water molecule interacts with the N–H and pyridine N sites in PxA, a result that confirms the conclusions about the D(SO···HO) dimer interaction with water. The zwitterionic tautomer forms a stable cyclic complex through C=O and O=SO groups interaction. The relative energy decreases comparing to the isolated tautomers. However, the stepwise water addition does not lead to substantial changes in the case of 2 and 3 water molecules, where complexes in both tautomers are built through hydrogen bonding of the solvent with SO_2 oxygen atoms. Finally after addition of the fourth water molecule the relative stability is reversed, showing PxZw more stable and describing the experimentally observed situation (Fig. 8 up).

Looking at the Px–water complexes, shown in Fig. 8 up, one should observe that the supramolecular structures are largely unbalanced. The $-SO_2$ and pyridine N-sites are hydrated, but the O–H···O= (PxA) or the O^-···H–N (PxZw) sites at opposite site of the solute remain without explicit water(s). A possible reason could be found in the steric hindrance coming from the neighbor aromatic hydrogen atoms and the fact that in both cases strong intramolecular hydrogen bonding is available.

Of course, this is a very simplified description of the solvent effect, which contains several problematic points: the stepwise procedure of water addition, which does not cover all possible variants at each step and, most importantly, the limited number of water molecules, which leads to neglecting solvent–solvent interactions and, therefore, forces them to interact with the solute attempting to form cyclic complexes.

In order to compensate the inborn defects of the bottom-up solvent effect description, a QM/MM procedure (as described in the Experimental part) was applied starting from 202 water

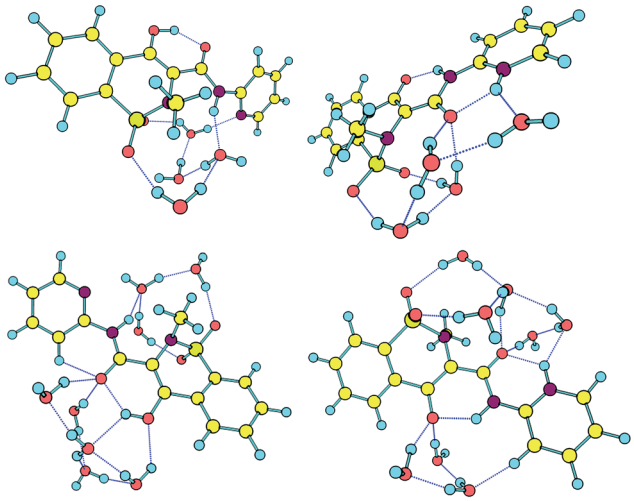

Fig. 8 Water complexes in water environment (M06-2X/TZVP, PCM solvent model) of PxA (left) and PxZw (right): top, bottom-up procedure (Table S4†), 4 water molecules; down, QM/MM based procedure, 8 water molecules.

molecules are solvent environment. Finally, the number of the solvent molecules was reduced to 10. At this solvent complex the PxZw is more stable with appr. 2 kcal mol^{-1}. The reduction of the water molecules to 8 and using only M06-2X/TZVP level of theory (Fig. 8 down) leads to relative energy‖ of −1.85 kcal mol^{-1}. This value is very near to the predicted in Table S4,† from one side, and to the value of Gibbs free energy extrapolated for pure water from the experimental data (−1.35 kcal mol^{-1}, Fig. S5†) and can be considered as an rough estimate of reality. A careful evaluation of complexes with 8 water molecules (Fig. 8 down) show that generally it is more difficult to hydrate the enol form, where the potentially strongly water attracting groups (C=O group and COH) are at the same side, while the zwitterionic form has two separated carbonyl groups, which makes them easier accessible for the surrounding water molecules. In fact, in the 8 water molecules complexes, shown in Fig. 8 down, the enol form directly interacts only with 7 of them, while the PxZw is bound directly to all. This fact, actually, can suggest that the description of the water effect needs separate investigation.

Experimental

Piroxicam was purchased from Fluka as European Pharmacopoeia reference standard and was used without additional purification.

Spectral measurements were performed on Jasco V-570 UV-Vis-NIR spectrophotometer, equipped with a thermostatic cell holder (using Huber MPC-K6 thermostat with precision 1 °C), in spectral grade solvents at 25 °C. The derivative spectra were calculated using the "step-by-step filter" as previously described.[30] The monomer–dimer equilibrium was studied according to ref. 21. The spectra in the binary ethanol–water and DMSO–water mixtures were analyzed by a quantitative procedure based on resolution of overlapping bands, which yields tautomeric molar fractions in each solution and the individual spectra of the single tautomers.[16,29]

The NMR spectra were recorded at a Varian Mercury 300 at 300 MHz for ^1H using ambient or low temperature. The solvents were both DMSO-d_6 and DMF-d_7. The solvent signals were used for internal referencing in such a way that it corresponded to the use of TMS.

Quantum-chemical calculations were performed by using the Gaussian 09 program suite[31] using M06-2X fitted hybrid meta-GGA functional[32] with TZVP basis set.[33] It is worth mentioning that this method has been recently demonstrated as very suitable for describing tautomeric behavior in azo-naphthols and related Schiff bases[34] as well as for prediction of the absorption spectra of organic dyes.[35,36]

The tautomeric forms of Px, their dimers and water complexes were optimized without restrictions in gas phase and in solvent medium under normal optimization conditions by using ultrafine grid in the computation of the two-electron integrals and their derivatives. The optimized structures were then characterized as true minima by vibrational frequency calculations. In all cases the solvent medium was described by using the PCM model, namely IEFPCM,[37] as implemented in Gaussian 09. The water box and the following molecular dynamics simulations (MM+ force field) were performed by using of HyperChem 8 Professional (Evaluation version).[38]

The specific effect of the water was modeled by two different procedures:

Bottom-up procedure: starting from isolated solute and then a stepwise addition of water molecules and optimizations of the overall complex in water medium without any restrictions. In this case, in order to reduce the computational efforts the next water molecule has been added to the most stable water–solute complex from the previous step. For instance, the complexes with two water molecules are based on the most stable structure with one water molecule (as shown in Table S4†) and the second water molecule has been added on all possible interacting sites looking for the most stable optimized structure.

Top-down approach: placing the solute in a water box (18 × 13 × 27 Å), containing 202 water molecules. Following the energy minimization procedure molecular dynamic simulations were performed by heating to 300 K and then equalization for 2 ns was carried out at constant pressure periodic boundary conditions. The complex was optimized by using QM/MM calculations[39] as implemented in Gaussian 09 (ONIOM[40]) using two layers, namely M06-2X/TZVP for the solute and UFF[41] for the water cloud. Then the number of the water molecules was reduced to 25, keeping only solvent molecules in near proximity of the solute, again optimized by QM/MM (the same conditions as above), but in water environment. In this complex only water molecules directly interacting with the solvent (now ten) remain in the next step, followed by consecutive M06-2X/TZVP:UFF and M06-2X/TZVP:M06-2X/SVP[33] optimization. From the resulting complex were removed these water molecules which do not interact directly with the tautomeric function sites and the oxygen atoms from SO_2 group and the

‖ Everywhere in the paper a positive relative energy means PxA more stable and *vice versa*.

complex was optimized by using M06-2X/TZVP level of theory. In all cases the water medium was approximated by using PCM solvent model.

Conclusions

Quantum-chemical calculations of the possible tautomers of Piroxicam have shown that two tautomers have potential to exist in solution: an enol-amide form and the zwitterion. The experimental investigations in solution by using UV-Vis and NMR spectroscopy have confirmed that the enol-amide tautomer is present in ethanol and in DMSO in both cases stabilized as sandwich type dimer. The corresponding dimerization constants have been determined as well. Upon addition of water the dimer is partially destroyed and the tautomeric equilibrium is shifted to the zwitterionic tautomer. The effect of the water environment in this process has been modeled by quantum chemical calculations showing good agreement with the experiment and stressing the importance of specific solute–solvent interactions.

Acknowledgements

The financial support from Bulgarian National Science Found (access to MADARA computer cluster by the project RNF01/0110) and Swiss National Science Found (SupraChem@Balkans.eu Institutional partnership project) is gratefully acknowledged. D.I. is indebted to the European Social Fund (BG051PO001-3.3.07-0002 Internships for university students project) for the internship at Bulgarian Academy of Sciences.

References

1 J. R. Vane, *Nat. New Biol.*, 1971, **231**, 232–235.
2 T. J. Schnitzer, J. M. Popovich, G. B. Andersson and T. P. Andriacchi, *Arthritis Rheum.*, 1993, **36**, 1207–1213.
3 D. L. Earnest, L. J. Hixson and D. S. Alberts, *J. Cell Biochem. Suppl.*, 1992, **16**, 156–166.
4 M. M. Wolfe, D. R. Lichtenstein and G. Singh, *N. Engl. J. Med.*, 1999, **340**, 1888–1899.
5 M. Gil and A. Douhal, *Chem. Phys.*, 2008, **350**, 179–185 and references cited therein.
6 M. El-Kemary, M. Gil and A. Douhal, *J. Med. Chem.*, 2007, **50**, 2896–2902.
7 R. Banerjee and M. Sarkar, *J. Lumin.*, 2002, **99**, 255–263.
8 A. R. Katritzky, C. D. Hall, B. El-Dien, M. El-Gendy and B. Draghici, *J. Comput.-Aided Mol. Des.*, 2010, **24**, 475–484.
9 (*a*) R.-S. Tsai, P.-A. Carrupt, N. El-Tayar, Y. Giroud, P. Andrade, B. Testa, F. Bree and J.-P. Tillement, *Helv. Chim. Acta*, 1993, **76**, 842–854; (*b*) P. Joliet, N. Simon, F. Bree, S. Urien, A. Pagliara, P. A. Carrupt, B. Testa and J. P. Tillement, *Pharm. Res.*, 1997, **14**, 650–656.
10 Px belongs to class II drugs (low aqueous solubility and high permeability, Biopharmaceutical Classification System according to the U.S. Food and Drug Administration).
11 (*a*) S. L. Childs and K. I. Hardcastle, *Cryst. Growth Des.*, 2007, **7**, 1291–1304 and references cited therein; (*b*) C. Wales, L. H. Thomas and C. C. Wilson, *CrystEngComm*, 2012, **14**, 7264–7274.
12 (*a*) A. R. Sheth, S. Bates, F. X. Muller and D. J. W. Grant, *Cryst. Growth Des.*, 2005, **5**, 571–578; (*b*) J. Bordner, J. A. Richards, P. Weeks and E. B. Whipple, *Acta Crystallogr., Sect. C: Cryst. Struct. Commun.*, 1984, **40**, 989–990; (*c*) A. Mishnev and G. Kiselovs, *Z. Naturforsch., B: J. Chem. Sci.*, 2013, **68**, 168–174.
13 S. M. Andrade and S. M. B. Costa, *Prog. Colloid Polym. Sci.*, 1996, **100**, 195–200.
14 Y. H. Kim, D. W. Cho, S. G. Kang, M. Yoon and D. Kim, *J. Lumin.*, 1994, **59**, 209–217.
15 (*a*) K. F. de Souza, J. A. Martins, F. B. T. Pessine and R. Custodio, *Spectrochim. Acta, Part A*, 2010, **75**, 901–907; (*b*) M. Franco-Perez, L. I. Reyes-Garcia, R. Moya-Hernandez and R. Gomez-Balderas, *Int. J. Quantum Chem.*, 2012, **112**, 3637–3645; (*c*) M. Franco-Perez, R. Moya-Hernandez, A. Rojas-Hernandez, A. Gutierrez and R. Gomez-Balderas, *J. Phys. Chem. B*, 2011, **115**, 13593–13598.
16 L. Antonov, Absorption UV-vis Spectroscopy and Chemometrics: From Qualitative Conclusions to Quantitative Analysis, *Tautomerism: Methods and Theories*, ed. L. Antonov, Wiley-VCH Verlag GmbH & Co. KGaA, 2013, ch. 2.
17 J. M. Geckle, D. M. Rescek and E. B. Whipple, *Magn. Reson. Chem.*, 1989, **27**, 150–154.
18 W. Liu, W. D. Wang, W. Wang, S. Bai and C. Dybowski, *J. Magn. Reson.*, 2010, **206**, 177–181.
19 (*a*) S. Bolvig and P. E. Hansen, *Magn. Reson. Chem.*, 1996, **34**, 467–478; (*b*) S. Bolvig and P. E. Hansen, *Curr. Org. Chem.*, 2000, **4**, 19–54; (*c*) A. Filarowski and P. E. Hansen, *Z. Phys. Chem.*, 2013, **227**, 917–927.
20 P. E. Hansen, Isotope Effects on Chemical Shifts as a Tool in the Study of Tautomeric Equilibria, *Tautomerism: Methods and Theories*, ed. L. Antonov, Wiley-VCH Verlag GmbH & Co. KGaA, 2013, ch. 6.
21 L. Antonov, G. Gergov, V. Petrov, M. Kubista and J. Nygren, *Talanta*, 1999, **49**, 99–106.
22 M. Kasha, H. R. Rawls and M. A. El-Bayomi, *Pure Appl. Chem.*, 1965, **11**, 371–392.
23 A. R. Sheth, S. Bates, F. X. Muller and D. J. W. Grant, *Cryst. Growth Des.*, 2005, **5**, 571–578; the CCDC codes for the corresponding cases are: BIYSEN04, BIYSEN05 and BIYSEN03.
24 (*a*) B. Kojic-Prodic and Z. Ruzic-Toros, *Acta Crystallogr., Sect. B: Struct. Crystallogr. Cryst. Chem.*, 1982, **38**, 2948–2951; (*b*) S. Il-Hwan, K. Kwang-Joo, K. Thong-Sung, K. Bong-Hee and C. K. Yong, *Chungnam J. Sci.*, 1989, **16**, 30; (*c*) K. Naelapaa, J. Van de Streek, J. Rantanen and A. D. Bond, *J. Pharm. Sci.*, 2012, **101**, 4214–4219.
25 G. Reck, G. Dietz, G. Laban, W. Gunther, G. Bannier and E. Hohne, *Pharmazie*, 1988, **43**, 477–481.
26 F. Vrecer, M. Vrbine and A. Meden, *Int. J. Pharm.*, 2003, **256**, 3–15.

27 M. Nyström, J. Roine, M. Murtomaa, R. M. Sankaran, H. A. Santos and J. Salonen, *Eur. J. Pharm. Biopharm.*, 2015, **89**, 182–189.
28 J. Bordner, J. A. Richards, P. Weeks and E. B. Whipple, *Acta Crystallogr., Sect. C: Cryst. Struct. Commun.*, 1984, **40**, 989–990.
29 (*a*) L. Antonov and D. Nedeltcheva, *Chem. Soc. Rev.*, 2000, **29**, 217–227; (*b*) L. Antonov and V. Pertov, *Anal. Bioanal. Chem.*, 2002, **374**, 1312–1317.
30 (*a*) L. Antonov, *Trends Anal. Chem.*, 1997, **16**, 536–543; (*b*) V. Petrov, L. Antonov, H. Ehara and N. Harada, *Comput. Chem.*, 2000, **24**, 561–569.
31 M. J. Frisch, G. W. Trucks, H. B. Schlegel, G. E. Scuseria, M. A. Robb, J. R. Cheeseman, G. Scalmani, V. Barone, B. Mennucci, G. A. Petersson, H. Nakatsuji, M. Caricato, X. Li, H. P. Hratchian, A. F. Izmaylov, J. Bloino, G. Zheng, J. L. Sonnenberg, M. Hada, M. Ehara, K. Toyota, R. Fukuda, J. Hasegawa, M. Ishida, T. Nakajima, Y. Honda, O. Kitao, H. Nakai, T. Vreven, J. A. Montgomery Jr, J. E. Peralta, F. Ogliaro, M. Bearpark, J. J. Heyd, E. Brothers, K. N. Kudin, V. N. Staroverov, R. Kobayashi, J. Normand, K. Raghavachari, A. Rendell, J. C. Burant, S. S. Iyengar, J. Tomasi, M. Cossi, N. Rega, J. M. Millam, M. Klene, J. E. Knox, J. B. Cross, V. Bakken, C. Adamo, J. Jaramillo, R. Gomperts, R. E. Stratmann, O. Yazyev, A. J. Austin, R. Cammi, C. Pomelli, J. W. Ochterski, R. L. Martin, K. Morokuma, V. G. Zakrzewski, G. A. Voth, P. Salvador, J. J. Dannenberg, S. Dapprich, A. D. Daniels, O. Farkas, J. B. Foresman, J. V. Ortiz, J. Cioslowski and D. J. Fox, *Gaussian 09, Revision A.02*, Gaussian, Inc., Wallingford CT, 2009.
32 (*a*) Y. Zhao and D. G. Truhlar, *Theor. Chem. Acc.*, 2008, **120**, 215–241; (*b*) Y. Zhao and D. G. Truhlar, *Acc. Chem. Res.*, 2008, **41**, 157–167.
33 F. Weigend and R. Ahlrichs, *Phys. Chem. Chem. Phys.*, 2005, **7**, 3297–3305.
34 S. Kawauchi and L. Antonov, *J. Phys. Org. Chem.*, 2013, **26**, 643–652.
35 See for details: A. Laurent, C. Adamo and D. Jacquemin, *Phys. Chem. Chem. Phys.*, 2014, **16**, 14334–14356.
36 (*a*) L. Antonov, V. Deneva, S. Simeonov, V. Kurteva, A. Crochet, K. M. Fromm, B. Shivachev, R. Nikolova, M. Savarese and C. Adamo, *ChemPhysChem*, 2015, **16**, 649–657; (*b*) S. Kawauchi, L. Antonov and Y. Okuno, *Bulg. Chem. Commun.*, 2014, **46A**, 228–237.
37 J. Tomasi, B. Mennucci and R. Cammi, *Chem. Rev.*, 2005, **105**, 2999–3093.
38 *HyperChem (TM) Professional 8.0*, Hypercube, Inc., 1115 NW 4th Street, Gainesville, Florida 32601, USA.
39 (*a*) S. D. Banik and A. Chandra, *J. Phys. Chem. B*, 2014, **118**, 11077–11089; (*b*) J. Gao, *Acc. Chem. Res.*, 1996, **29**, 298–305; (*c*) P. I. Nagy, G. Alagona and C. Ghio, *J. Chem. Theory Comput.*, 2007, **3**, 1249–1266.
40 S. Dapprich, I. Komáromi, K. S. Byun, K. Morokuma and M. J. Frisch, *J. Mol. Struct.: THEOCHEM*, 1999, **462**, 1–21.
41 A. K. Rappé, C. J. Casewit, K. S. Colwell, W. A. Goddart and W. M. Skiff, *J. Am. Chem. Soc.*, 1992, **114**, 10024–10035.